Egypt. J. Chem. **Vol. 65,** No. SI: 13B pp. 181 - 194 (2022)

Egyptian Journal of Chemistry

http://ejchem.journals.ekb.eg/

Production and Evaluation of Fortified Biscuit with Iron Nanoparticles for Anemia as Functional Food

Alaa G. Osman[1, 2], Ahmed I. El-Desouky[1], Mohamed K. Morsy[*1], Ahmed A. Aboud[3], Mahmoud H. Mohamed[1*]

[1] *Department of Food Technology, Faculty of Agriculture, Benha University, 13736, Qaluobia, Egypt.*
[2]*Academy of Scientific Research and Technology (ASRT), 11516, Cairo, Egypt.*
[3]*Department of Physics, Faculty of Science, Beni-Suef University, 62521, Beni-Suef, Egypt.*

Abstract

Biscuits are favored products for people of different ages world-wide due to its high-energy foods, long shelf-life, and easy absorption. This study aimed to evaluate the fortified biscuit with iron nanoparticles (Fe_2O_3-NPs) as novel approach to overcome iron deficiency anemia (IDA) disease. In preliminary experiments, we utilized 4 groups of albino rats as follows; negative group (G1; control), positive group (G2), treated anemic group (G3), and untreated anemic group (G4). The SEM, XRD, histopathological, and hematology tests were performed. The results revealed that the Fe_2O_3-NPs was at 49.5±5 nm, homogenous, and purity. Fortified biscuits with Fe_2O_3-NPs increased the iron level (289±1.0 mg/dL), red blood counts (9.1±0.2 10^{12}/L), and hemoglobin (18±0.25 g/dL) in the G3 compared to other groups. Histological examination showed that no significant effects on the spleen, kidney, and liver. Results demonstrated that the fortified biscuit with Fe_2O_3-NPs (10 ppm) at 49.5±5 nm is more effective in IDA treatment.

Key words: Iron deficiency anemia, nanoparticles, albino rats, hematology analysis, histopathological examination

1. Introduction

Iron deficiency anemia (IDA) is one of the most wide-spread pathological states common nutritional deficiency health disorders, and social problems for children, elderly, and women [1-2]. According to WHO reported that the prevalence of IDA is 8% of preschool children, 15% of pregnant women and 12% of non-pregnant women, and 5% of men while, in Egypt, there are 31% of preschool children, 22% of pregnant, and 28% of women [3]. The IDA happens due to some factors i.e. (i) decrease in iron daily intake, (ii) malabsorption of iron, and (iii) increased demand for iron [4]. Recently, the IDA has been linked with infection with coronavirus disease (COVID-19).

Nowadays, COVID-19 is common pathogens disease caused by SARS-COV2, it is world-wide spread from Wuhan, China [5-6]. COVID-19 pandemic infects the immune system, hemoglobin, and red blood counts [7]. According to the recent reports, the COVID-19 reduces heme-iron and hemoglobin metabolism in humans based on some mechanisms as follows (i) linking the beta-chains on glycoproteins surface and desaturate it [8]. (ii) Produces mimicry hepcidin which links with ferroportin which decreases iron absorption, metabolism ultimately, and ferroptosis hyperferritinemia [8]. WHO estimated globally illness patients by COVID-19 over than 129 million and 2.81 million deaths cases, while in Egypt about 202,699 illness cases and 12,025 deaths cases, [9].

Iron is considered an important dietary and health element in humans such as O_2 transport, DNA, red blood cells and hemoglobin synthesis, ATP production, steroid synthesis, and electron transport [10-11]. One study by [12] recommended the daily intake of iron for the human body is 10 - 15 mg and the absorption ratio 30:35%. The ferric (Fe III) irons are absorbed in enterocytes by metal transporter 1 (DMT1) and convert to ferrous (Fe II) by cytochrome b and duodenal [13]. Heme-iron carried into enterocytes and degraded by heme oxygenase-1 (HO-1) [14] to Fe (II) [15]. Hephaestin oxidized Fe (II) to Fe (III) resulting Fe (II) ions bounded to transferrin serum [15]. There are various traditional oral iron salts i.e. iron sulfate and iron fumarate, however, it takes a long time to store iron, low absorption in the body, and gastrointestinal bad effects [16-17]. The strategy for increasing the iron absorption changes the iron shape, size, and coated it with other materials such as organic

*Corresponding author e-mail: mohamed.abdelhafez@fagr.bu.edu.eg.; (gggggggggggggggggggg).
Receive Date: 27 January 2022, Revise Date: 27 February 2022, Accept Date: 21 March 2022
DOI: 10.21608/EJCHEM.2022.118578.5338

acids [18]. Nanotechnology is offering new opportunities for innovative functional and safe foods for humans and protect them from diseases [19]. Nanotechnology was increased nutrients bioavailability, great efficiency, low side effects, and high absorption, so its need to lower doses compared with traditional drugs [20-21]

The fortified foods enriched with iron very important to meet the daily dose of iron requirements and enhance the iron role in the body especially for preschool children, pregnant, and elderly [22]. Biscuit is the most common cereal product among the people around the world [23]. That is revert to different sensory parameters, low cost, high nutrition, easy absorption, and long shelf life [24].

The recent investigations presented iron oxide nanoparticles (27 ppm) at 6.22–9.7 and 64–68 nm, respectively for 8 weeks were increased the levels of red blood counts, hemoglobin, mean cell volume, mean cell hemoglobin concentration, and iron in anemic albino rats induced by lead acetate [25]. Another research estimated the supplementation of nano-iron oxide at 6 mg for 23 days showed no bad effects and toxic on the organs, improved the hematology and serum analysis [26].

All scientists worldwide do their best to improve and develop the traditional food products for IDA treatment. At the same time, the nutrition researchers try very hard to find a functional food to increase the iron level in blood and treatment the IDA. This study was aimed to (i) produce and evaluate fortified biscuit with nano-iron, and (ii) study the effects of functional biscuit on hematology, histopathological analysis, and growth performance.

2. Materials and Methods

2.1. Raw materials and chemicals

Iron chloride, sodium bicarbonate, ascorbic acid, and phenylhydrazine were purchased from El-Nasser Company, Cairo, Egypt. The basal diet ingredients (starch 67%, casein 15%, corn oil 7%, cellulose 5%, minerals 4%, and vitamins 2%,) were supplied from Egypt Lab Company, Cairo, Egypt. Raw chocolate and butter were purchased from the local market at Benha, Qaluobia, Egypt. Wheat flour 72%, sugar, skim milk powder, baking powder, vanilla powder, salt, margarine, and eggs were purchased from the local market at Benha, Qaluobia, Egypt.

2.2. Preparation of iron oxide nanoparticles (Fe_2O_3-NPs)

Iron oxide nanoparticle was prepared according to the method described by (Salah and Regheb 2016), [27]. Briefly, iron chloride (0.54g/15 mL; *w/v*) and sodium carbonate (0.6g/10 mL; *w/v*) were dissolved in distilled water. The solutions were mixed for 15 min at 1000 rpm/min till brown color appearance. Ascorbic acid (0.12 g) was added directly with stirring for 15 min at 1000 rpm/min and the brown color turn into black color. The solution was put in the oven at 160°C for 3 h and centrifuged for 5 min at 2500 rpm/min. Iron nanoparticles were put in the oven at 60ºC to dry and kept in a dark glass bottle till used.

2.3. Analytical characterization of iron oxide nanoparticles (Fe_2O_3-NPs)

2.3.1 X- Ray diffraction (XRD)

The X-ray diffraction (XRD) of Fe_2O_3-NPs was measured using X-ray diffractometer (Rigaku D/Max-B, Tokyo, Japan) according to [28]. The samples were put onto a glass slide and the spectra were recorded using Cu radiation (wavelength of 0.1541 nm) and a nickel monochromator filtering wave at 40 kV and 30 mA. The average crystallite size of Fe_2O_3-NPs was estimated using Scherer's equation $D = \frac{k\lambda}{\beta cos\theta}$ [29]. Where D is the particle size, k is a constant equal 0.9, λ is the X-ray beam wavelength (1.54 Å), β is the full width at half maximum and θ is the center of the diffraction peak.

2.3.2. Scanning electron microscope (SEM)

The SEM of Fe_2O_3-NPs was measured (JSM-6510-LA Ja, Japan) according to [30]. The powder was put onto aluminum specimen stubs using double-stick carbon tabs and plated by palladium/gold on an ion sputter coated for 45 s at 20 mA. The powder was checked using an accelerating beam at a voltage of 1.5 kV. Magnifications of SEM at 40,000 and 60,000 were used.

2.3. Preparation of fortified biscuit

The biscuit coated with chocolate including Fe_2O_3-NPs was prepared according to the method described by [24] with slight modifications. In brief, the dry components i.e. (wheat flour 220g, sugar 50g, dried milk 25g, baking powder 1.5g, vanilla 1g, and salt 1.5g) were mixed for 90 s. The wet ingredients i.e. (water 15 mL, margarine 80g, and eggs 20g) mixed and added to the previous dry dough and blend for 3 min. The dough spread, formed, cut at the size 40 mm, and backed at 180ºC for 30 min and cooled at 25±1°C for 60 min. Raw chocolate and butter were melted together at 40ºC, and Fe_2O_3-NPs at (10 ppm / 20g biscuit) were added directly to the previous solution and stirred at 1500 rpm/min for 15 min. The chocolate included Fe_2O_3-NPs used to coat the biscuit at 9 mm thickness and solid at 5±1°C for 100 min and packaged in polyethylene till utilized in feeding experiments.

2.4. Chemical analysis and sensory evaluation of fortified biscuit with nano-iron

The chemical analysis of fortified biscuit i.e. carbohydrate, protein, moisture, fiber, fat, and ash contents were determined according to the methods

described by [31]. The sensory properties of fortified biscuit were evaluated by 10 expert panelists at Food Technology Dept., Fac. of Agric., Benha Uni., Egypt. Panelists evaluated the biscuit parameters included all over acceptance, appearance, color, odor, and texture using a 5-point hedonic scale (1=extremely disliked; 5=extremely liked) according to [23].

2.5. Biological experiments

The design of biological experiment

Albino male rats at 6 weeks old were obtained from Animal House, Agricultural Research Center (ARC), Giza, Egypt. Rats were adapted for 4 days, split into 4 groups (6 rats/group), kept in filter-top polycarbonate cages at 28±1ºC, 50-70% RH, 12 h light:12 h dark, and the room free of any contamination source. Rats in different groups were fed on 20 g daily and drunk distilled water for 6 weeks as shown in **Table (1).** Twenty four male albino rats at 6 weeks old (6 rats /group) were utilized in this research as follow; group fed on the biscuit with chocolate (G1), group fed on basal diet (G2), treated anemic group fed on biscuit coated with chocolate incorporated with nano-iron (G3), and the untreated group fed on basal diet free of iron element (G4) to determine the influence of functional biscuit with Fe_2O_3-NPs on the iron level in blood and improve iron deficiency anemia (IDA). As well, the serum and hematology analyses, measurement of the growth rate, and histopathological analysis were done.

Table 1: Design of biological experiment to evaluate the effect of fortified biscuit with nano-iron (Fe_2O_3-NPs) on iron level in albino rats

	(G1)	(G2)	(G3)	(G4)
Casein (g)	5.1	15	5.1	5.1
Salt mixture (g)	8.2	4	8.2 Free of iron	8.2 Free of iron
Vitamin mixture (g)	3.6	2	3.6	3.6
Cellulose (g)	4.5	5	4.5	4.5
Corn oil (g)	-	7	-	-
Starch (g)	-	67	-	-
Biscuit coated with chocolate (g)	79	-	79	79
Iron oxide nanoparticles (ppm)	-	-	50 ppm	-

2.5.1. Inducing anemia in albino rats

Anemia was induced by venoclysis in rat tails for 4 days at a concentration of 10 mg/kg using melted phenyl hydrazine in sterilized normal saline for groups (3 and 4) according to [32].

2.5.2. Effect of biscuit enriched with nano-iron on growth performance

The body gain weight of rats was evaluated according to [33]. The weight gain of rats measured according to the following equation; (WBG)=[(FBW-IBW)/IBW] ×100, where WBG is weight body gain, FBW is final body weight, and IBW is initial body weight.

2.5.3. Serum and hematology analyses

The blood samples were gathered and tested at the start, mid, and the end of the biological experiment (6 weeks). Cell blood counts (CBCs), total iron-binding capacity (TIBC), transferrin, total iron, total protein, sodium, potassium, reticulocyte counts, and γ - glutamyl transferase (GGT) were determined according to [32; 34-36]

2.5.4. Kidney and liver functions

Uric acid, urea, and creatinine were tested by the kit colorimetric enzyme assay according to [37]. Alkaline phosphatase (ALP), total bilirubin, albumin, glutamic pyruvic transaminase (GPT), and glutamic oxaloacetic transaminase (GOT) were done in serum according to [38].

2.6. Histopathological examination of albino rats

Histopathological examination of rat's organ was prepared at Oncology Hospital, Tanta, Egypt. Rats were sacrificed at the end of the designated period. Liver, spleen, and kidneys were removed from each animal and immersion-fixed in 10 % formalin solution at room temperature 25±1ºC for 12 h. Serial dilutions of methyl alcohol were used. Specimens were cleared in xylene embedded in paraffin at 56ºC in a hot air oven for 24 h. Paraffin bees wax tissue blocks were prepared for sectioning at 4-micron thickness by slide microtome. The obtained tissue sections were collected on glass slides, deparaffinized, stained by hematoxylin and eosin (H & E), and subsequently processed for histopathological examination under the light microscope (Leica DM1000, Germany) as reported by [34].

2.7. Statistical analysis

The results were statistically analyzed using ANOVA one-way with a significate value of ($p \leq 0.05$) by SPSS software, var. 18 (IBM; Armonk, N.Y., U.S.A.). Results were investigated as a completely randomized design according to [39].

3. Results

3.1. Characterization of iron oxide nanoparticles (Fe_2O_3-NPs)

3.1.1. X-ray diffraction (XRD)

Iron oxide nanoparticles (Fe_2O_3-NPs) were measured by XRD to determine the crystallite size and the purity of the powder. As shown in **(**Figure 1 a) the

XRD pattern of dry Fe_2O_3-NPs powder was high purity, clear and broad peaks. The XRD pattern fits well with a brownish-black pyramidal crystal structure and the average crystal (diameter). The width of the peak matched with the small size of Fe_2O_3-NPs. Therefore, the results of XRD characterization concluded the crystallite size 49±5 nm.

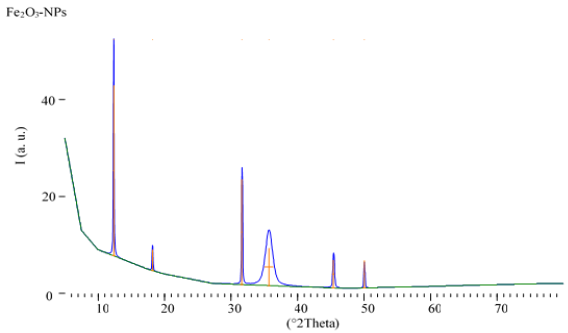

Fig. (1 a): X-ray diffraction (XRD) of iron oxide nanoparticles (Fe_2O_3-NPs).

3.1.2. Scanning electron microscope (SEM)

Figure (1 b) presented Fe_2O_3-NPs morphological characteristics. The size was evaluated by ImageJ program software.

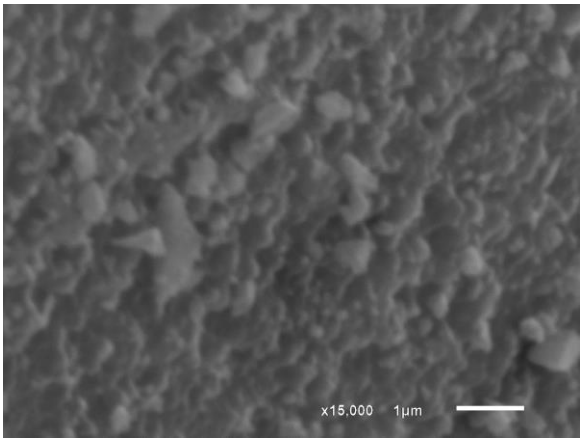

Fig. (1 b): Scanning electron microscope (SEM) of iron oxide nanoparticles (Fe_2O_3-NPs).

3.2. Chemical analysis and sensory evaluation of fortified biscuit with nano-iron

The main cause to choose biscuit back to enrich with nutritional elements, prefer to children and elderly, and easy absorption. Table (2) showed that fortified biscuit has highly nutritive value i.e. carbohydrate (62.5±0.2g), protein (9±0.3g), fat (17±0.17g), fiber (4.5±0.31g), moisture (5.2±0.2g), ash (1.8±0.16g), iron (12.01±0.1mg), calcium (15.30±0.10mg), and sodium (66.48± 0.11mg). Also, the sensorial evaluation was evaluated, and the results demonstrated there were non-significant differences ($p \geq 0.05$) between the fortified biscuit coated with chocolate incorporated Fe_2O_3-NPs samples as illustrated in Table (2). These data are similar to those illustrated by [24; 40]

Table 2 Chemical composition and sensorial evaluation of biscuit coated with chocolate with/free of nano-iron (per g/100g) on dry weight basis.

	Values	
Quality attributes	Biscuit coated with chocolate	Biscuit coated with chocolate enriched with nano-iron
Carbohydrate(g)	62.2±0.18 [a]	62.5±0.2 [a]
Fat (g)	17±0.18 [a]	17±0.17 [a]
Protein (g)	9±0.19 [a]	9±0.3 [a]
Moisture (g)	5.8±0.1 [a]	5.2±0.2 [b]
Fiber (g)	4.5±0.21 [a]	4.5±0.31 [a]
Ash (g)	1.5±0.12 [b]	1.8±0.16 [a]
Iron (mg)	1.68± 0.03[b]	12.01±0.1 [a]
Sodium (mg)	62.68± 0.11[b]	66.48± 0.11 [a]
Calcium (mg)	12.10± 0.10[b]	15.30± 0.10 [a]
Sensorial parameters	Values	
Texture	5±0.16 [a]	5±0.1 [a]
Appearance	4±0.12 [b]	4.5±0.21 a
Odor	5±0.21 [a]	4.8±0.16 [b]
Color	4.5±0.12 [a]	4.3±0.3 [b]
All over acceptance	4.5±0.1 [b]	6±0.12 [a]

3.3. Hematology analysis and growth evaluation

3.3.1. Effect of fortified biscuit with nano-iron on growth performance

The weight of albino rats was done every week. G4 was a low weight gain rate during the feeding of the experiment period compared with other groups as shown in Figure (2).

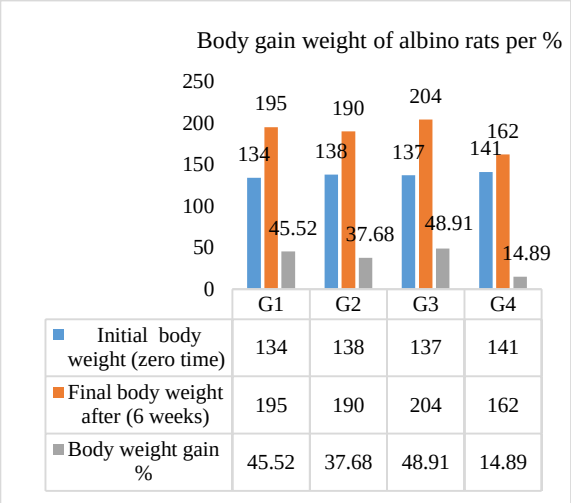

3.3.2. Cell blood counts (CBCs)

Cell blood counts (CBCs) included e.g. red blood counts (RBCs), white blood counts (WBCs), hemoglobin (Hb), mean cell volume (MCV), mean cell hemoglobin (MCH), mean cell hemoglobin concentration (MCHC), and platelets count (PLTs) were determined. As shown in Table (3), the RBCs, WBCs, Hb, MCV, MCH, MCHC, and PLTs were almost stable values in groups 1and 2 during the feeding experiment periods. While, these parameters were increased gradually till become at normal levels during the feeding period in group 3. The normal levels of these parameters are 4.3:5.9 x 10^{12}/L, 4.5:11.0 x 10^{9}/L, 12.0:16.0 g/dL, 80:100 fl, 25.4 :34.6 pg, 31:36 g/dL, and 150:400 x 10^{9}/L, respectively. On the other hand, these parameters were less level in G4.

The serum analyses such as total iron capacity (TIBC), transferrin (Tf), total iron (TI), total protein (TP), sodium (Na), potassium (K), reticulocyte counts (RCs), and γ -glutamyl transferase (GGT) were determined, in Table (4). The obtained results showed that, in groups (G1, G2, and G3) the TIBC and transferrin nearly to the normal values during the feeding experiments period. While, there were gradually increasing levels of TIBC, Tf, RCs, and GGT increasing during the feeding experiments period in G4. The normal values are 240:450 mcg/dL, 40:45 mcg/dL, 60:170 mcg/dL, 6:8.3 g/L, 134:145 mEq/L, 5.1:6.0 mEq/L, 2:6×10^{9}/L, and 9:48 U/L The elevated level referred to highly iron deficiency anemia due to the non-availability of iron absorption. On the other side, TI, TP, Na, K values were gradually elevated in G1, G2, and G3 during the feeding experiments period, while there were gradually levels decreasing in G4.

3.3.4. Kidney function parameters

The kidney functions such as urea, uric acid, and creatinine were evaluated. In Table (5) the results showed that there were significant differences between G4 and other groups. Moreover, there were a gradual increase in urea, uric acid, and creatinine values in G4 compared to other groups. The normal values of these parameters are 35:50 mg/dL, 3.4:7.0 mg/dL and 0.6:1.2 mg/dL.

3.3.3. Serum analyses determination in albino rats

3.3.5. Liver function parameters

The liver functions i.e. albumin, Alkaline phosphatase (ALP), glutamic oxaloacetic transaminase (GOT or ALT), glutamic pyruvic transaminase (GPT or AST), and total bilirubin were determined. Table (6) illustrated that, in G4 there was an increasing value of albumin, ALP, GOT, GPT, and total bilirubin compared with other groups (1, 2, and 3) during the experiments period. The normal levels were 3.5:5.0 g/dL, 45:115 U/L, 7:55 U/L, 8:48 U/L, and 0.1:1.2 mg/dL.

3.4. Histopathological examination

3.4.1. Effect of fortified biscuit and basal diet on rats

There are no histopathological changes were observed in the examined organs of G1 and G2 as shown in Figure (3 a, b, c). The liver showed normal histological appearance of hepatic blood vessels with occasional mild activation of Kupffer cells and hepatocytes. As well, the kidney revealed normal histological criteria of glomeruli and renal convoluted tubules. In addition, the spleen exhibited normal white and red pulp with occasional hyperplasia and activation of reticuloendothelial cells of white pulp.

Table 3: Cell blood counts determination of albino rats during feeding on fortified biscuit with nano-iron (Fe_2O_3-NPs).

	Groups	Normal

Cell blood counts (CBCs) parameters	G1		G2		G3		G4		
	Before feeding	After feeding	Before feeding	After feeding	Before feeding	After feeding	Before feeding	After feeding	
Red blood counts (RBCs) (10^{12}/L)	6.6±0.28^{b}	6.9±0.36^{b}	6.4±0.26^{b}	6.2±0.4^{b}	3.8±0.3^{c}	7.1±0.2^{a}	3.6±0.15^{c}	5.1±0.2^{b}	4.3:5.9
Hemoglobin (Hb) (g/dL)	13.6±0.4^{c}	15.9±0.86^{b}	14±0.25^{c}	14.9±0.26^{b}	5±0.5^{e}	16±0.25^{a}	4.5±0.11^{e}	7.6±0.41^{d}	12.0:16.0
Mean cell hemoglobin (MCH) (pg)	24.4±0.3^{a}	22.9±0.7^{c}	23.3±0.5^{b}	22.7±0.4^{c}	12.8±0.6^{d}	22.6±0.7^{c}	12.5±0.1^{d}	10.8±0.4^{e}	25.4:34.6
White blood counts (WBCs) (10^{9}/L)	5.9±0.2^{b}	4.0±0.15^{c}	6.6±0.2 ^{a}	4.7±0.5^{c}	5.1±0.2^{b}	6.1±0.25^{a}	5.1±0.1^{b}	3.3±0.05^{d}	4.5:11.0
Mean cell volume (MCV) (fl)	65±0.8^{a}	62±0.8^{b}	63±0.35^{b}	68±0.9^{a}	49±0.5^{d}	59±0.7^{c}	46±0.52^{d}	44±0.9^{d}	80:100
Mean cell hemoglobin concentration (MCHC) (g/dL)	36±0.4^{b}	36±0.8^{b}	35±0.3^{b}	33±0.6^{c}	28±0.9^{d}	40±0.7 ^{a}	27±0.8^{d}	29±1.0^{d}	31:36
Platelets count (PLT) (10^{9}/L)	605±2^{c}	614±3.1^{c}	600±1.5^{c}	610±2.1^{c}	1559±2.5 ^{a}	662±2.1^{c}	1686±2.1 ^{a}	710±3.1^{b}	750:1000

Table 4: Serum analyses of albino rats during feeding on biscuit enriched with nano-iron (Fe_2O_3-NPs)

Serum analysis	Groups								Normal
	G1		G2		G3		G4		
	Before feeding	After feeding	Before feeding	After feeding	Before feeding	After feeding	Before feeding	After feeding	
Iron (I) (mg/dL)	216±3.5^{c}	288±2.0^{a}	210±5.0^{c}	275±4.5^{b}	215±5.0^{c}	289±1.0^{a}	205±4.5^{d}	185±4.5^{e}	60:170
Total protein (TP) (g/dL)	7.2±0.2^{b}	8.32±0.2^{a}	7.1±0.3^{b}	8.4±0.1^{a}	7.0±0.2^{b}	8.9±0.9^{a}	6.6±0.3^{c}	5.6±0.3^{d}	6:8.3
γ -glutamyl transferase (GGT) (U/L)	9.8±0.3^{a}	3.5±0.5^{c}	9.1±0.2^{a}	2.1±0.2^{d}	8.3±0.3^{b}	2.5±0.5^{d}	8.3±0.3^{b}	8.3±0.3^{b}	9:48
Sodium (Na) (mEq/L)	136±2.1^{b}	141±0.9^{a}	135±1.5^{b}	143±1.0^{a}	134±2.0^{b}	143±1.6^{a}	134±1.0^{b}	114±3.5^{c}	134:145
Potassium (K) (mEq/L)	6.0±0.2^{b}	6.4±0.9^{a}	6.4±0.1^{a}	6.9±0.3 ^{a}	5.8±0.1^{c}	6.4±0.1^{a}	5.7±0.2^{c}	4.5±0.4^{d}	5.1:6.0
Reticulate counts (RC) (10^{9}/L)	2.9±0.2^{c}	4.9±0.6^{b}	2.5±0.2^{c}	4.6±0.4^{b}	2.6±0.3^{c}	4.5±0.4^{b}	2.7±0.1^{c}	6.4±0.3^{a}	2:6
Total iron binding capacity (TIBC) (mcg/dL)	506±3.1^{d}	597±5.0^{b}	513±1.5^{d}	594±4.2^{b}	504±4.0^{d}	554±4.0^{c}	515±4.5^{d}	717±2.0^{a}	240:450
Transferrin (Tf) (mg/dL)	30.7±0.6^{d}	43.3±2.0^{b}	34.4±0.6^{d}	42.2±0.7^{b}	32.3±1.2^{d}	40.3±1.0^{c}	30.5±1.8^{d}	61.5±0.8^{a}	40:45

Table 5: Kidney function parameters of albino rats during feeding on fortified biscuit with nano-iron (Fe_2O_3-NPs)

Kidney function parameters	Groups								Normal
	G1		G2		G3		G4		
	Before feeding	After feeding	Before feeding	After feeding	Before feeding	After feeding	Before feeding	After feeding	
Urea (mg/dL)	49.8±0.8^{c}	42.6±0.7^{d}	51.2±0.6^{b}	45.1±1.0 ^{a}	49.4±0.6^{c}	40.2±0.9^{d}	48±1.0 ^{a}	58.4±1.2^{a}	35:50
Uric acid (mg/dL)	4.3±0.2^{d}	5.0±0.4^{a}	5.1±0.3^{a}	4.4±0.4^{c}	4.6±0.4^{b}	4.4±0.5^{c}	4.4±0.4^{c}	5.1±0.3^{a}	3.4:7.0
Creatinine (mg/dL)	1.0±0.10^{a}	0.75±0.05^{c}	0.9±0.05^{b}	0.82±0.02^{b}	0.8±0.03^{b}	0.45±0.01^{d}	0.8±0.01^{b}	1.15±0.16^{a}	0.6:1.2

Table 6: Liver function parameters of albino rats during feeding on fortified biscuit with nano-iron (Fe_2O_3-NPs)

Liver functic parameters	Groups								Normal
	G1		G2		G3		G4		
	Before feeding	After feeding	Before feeding	After feeding	Before feeding	After feeding	Before feeding	After feeding	
Glutamic oxaloacetic transaminase (GOT) (U/L)	77±1^{a}	63±1^{c}	70±1^{b}	58±0.8^{d}	66.8±0.8^{d}	58±1^{a}	70±2.6^{b}	77±0.6^{a}	47:75

glutamic pyruvic transaminase (GPT) (U/L)	30±1^{b}	18.7±2^{e}	33.3±2^{b}	21.7±2^{d}	28±1^{c}	18±1^{e}	35.3±2^{a}	40.2±1^{a}	8:48
Alkaline phosphatase ALP (U/L)	294±3.9^{a}	256±3.3^{c}	277.9±2.2^{b}	254.5±4.5^{c}	265.7±2.5^{c}	243.6±1.8^{d}	268.3±4.2^{c}	297.3±0.3^{a}	245:315
Total bilirubin (TB) (mg/dL)	0.75±0.02^{d}	0.93±0.03^{b}	0.75±0.05^{d}	0.94±0.02^{b}	0.72±0.01^{d}	0.86±0.03^{c}	0.73±0.03^{d}	1.25±0.04^{a}	0.1:1.2
Albumin (g/dL)	4.36±0.2^{b}	4.02±0.1^{d}	4.20±0.2^{c}	3.97±0.1^{d}	4.20±0.2^{c}	4.07±0.2^{d}	4.37±0.2^{b}	5.37±0.5^{a}	3.5:5.0

3.4.2. Impact of fortified biscuit with nano-iron on anemic rats

According to Figure (4 a, b, c, d, e), the microscopical examination of the livers revealed dilatation and congestion of central and portal veins. Random areas of coagulative necrosis characterized by loss of cellular detail of hepatocytes and retention of tissue architecture with shrunken hypereosinophilic cytoplasm and pyknotic nuclei were observed. Rarely, there were lytic areas of Hepatocellular necrosis, with loss of cord architecture and replaced by mixed inflammatory cells, fibrin, and small amounts of eosinophilic cellular and karyorrhectic debris. Portal areas were moderately expanded by increased numbers of small bile ducts (biliary ductal reaction), fibrin, and edema admixed with low to moderate numbers of mononuclear inflammatory cells and reactive fibroblasts. The examined kidneys revealed mild cloudy swelling, vacuolar and hydropic degeneration of lining epithelium of proximal and distal convoluted tubules in the renal cortex. Rarely, the lining epithelium of renal tubules exhibited coagulative necrosis characterized by retention of tubular architecture with hypereosinophilic cytoplasm and pyknosis of nuclei. The spleen showed moderate lymphoid depletion characterized by a loosely defined focus of cells in the white pulp that were differentiated by reduced cellular density than the greater proportion of small cells of the surrounding.

G1: Group 1 (feeding on biscuit coated with chocolate)

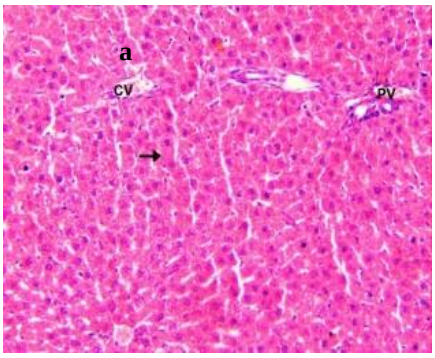

(a): Liver of rat showing normal histological appearance of central (CV), portal veins (PV) and hepatocytes (arrow). H&E stain x 200

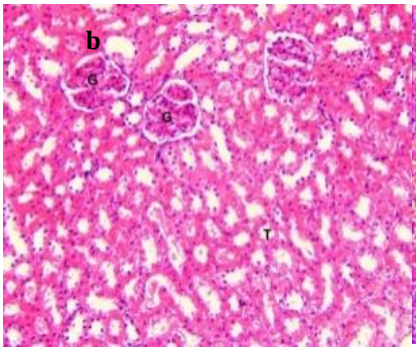

(b): Kidney of rat showing normal histological criteria of glomeruli (G) and renal convoluted tubules (T). H&E stain x 200

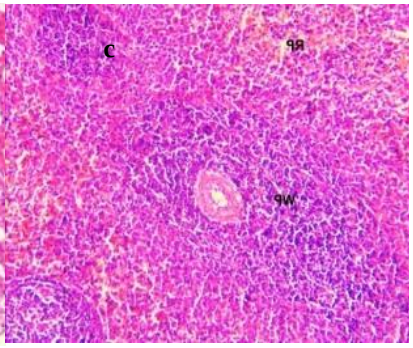

(c): Spleen of rat showing normal white (WP) and red pulp (RP). H&E stain x 200

G2: Group 2(feeding on normal basal diet)

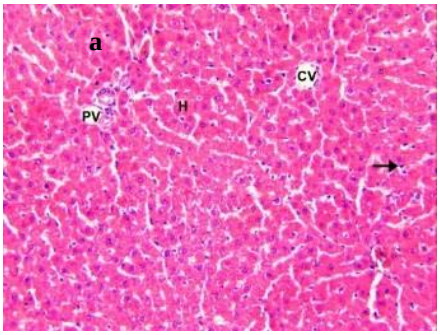

(a): Liver of rat showing histological appearance of hepatocytes (H), central (CV) and portal veins (PV) with mild activation of Kupffer cells (arrow). H&E stain x 200.

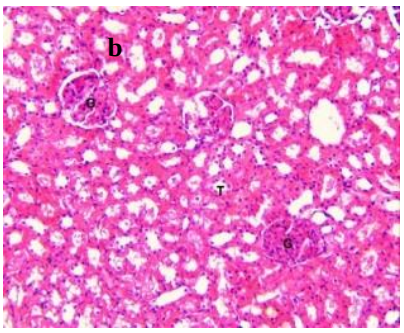

(b): Kidney of rat showing normal histological criteria of glomeruli (G) and renal convoluted tubules (T). H&E stain x 200.

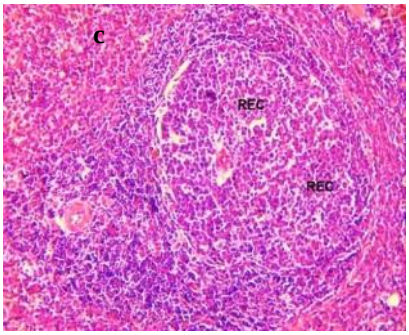

(c): Spleen of rat showing hyperplasia and activation of reticuloendothelial cells (REC) of white pulp. H&E stain x 200.

Fig. (3): Histological examination of rat's organ fed on basal diet and experimental biscuit coated with chocolate for 6 weeks.

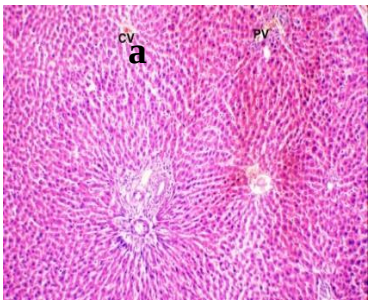

(a): Liver of iron-deficient rat showing dilatation and congestion of central (CV) and portal veins (PV). H&E stain x 100.

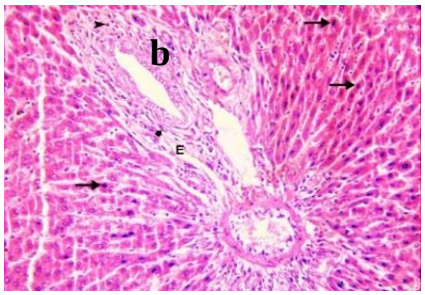

(b): Liver of iron-deficient rat showing coagulative necrosis of hepatocytes characterized by and retention of tissue architecture with shrunken hyper eosinophilic cytoplasm and pyknotic nuclei (arrow). Note also portal edema (E) admixed with mononuclear inflammatory cells (arrowhead) and reactive fibroblasts (thick arrow). H&E stain x 200.

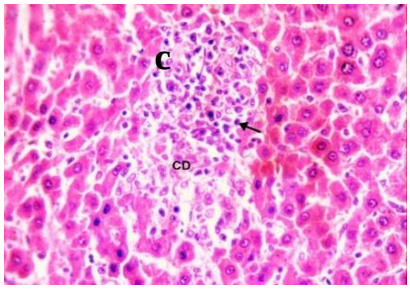

(c): Liver of iron-deficient rat showing lytic necrosis, with loss of cord architecture and replaced by mixed inflammatory cells (arrow), fibrin and eosinophilic cellular debris (CD). H&E stain x 200.

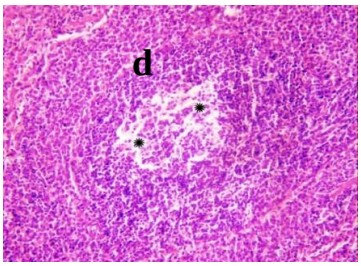

(e): Kidney of iron-deficient showing moderate lymphoid depletion (asterisk) characterized by a loosely defined focus of cells in the white pulp. H&E stain x 200.

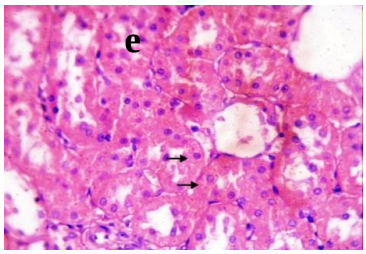

(d): Kidney of iron-deficient rat showing mild cloudy swelling (arrow) of lining epithelium of proximal and distal convoluted tubules. H&E stain x 400.

Fig. (4): Effect of feeding experimental fortified biscuit with nano-iron on spleen, kidney, and liver in anemic group (G3) during feeding period for 6 weeks.

3.4.3. Effect of basal diet on anemic rats

As shown in Figure (5 a, b, c, d, e, f, g, h, i, j, k, l, m, n), the microscopical examination of the livers revealed marked dilatation and congestion of central and portal veins. Multifocally, there were large fibrin thrombi attached to tunica intima and partially occluded the lumen of central and portal veins. Randomly scattered throughout the parenchyma were discrete, areas of coagulative necrosis characterized by loss of cellular detail of hepatocytes and retention of tissue architecture with shrunken hypereosinophilic cytoplasm and pyknotic nuclei. Occasionally, there were other areas of Hepatocellular necrosis, with loss of cord architecture and replaced by macrophages, lymphocytes, neutrophils, fibrin, and small amounts of eosinophilic cellular and karyorrhectic debris. Portal areas were moderately expanded by increased numbers of small bile ducts (biliary ductal reaction), edema, fibrin, and frequently contain low to moderate numbers of mononuclear inflammatory cells and reactive fibroblasts. The examined kidneys revealed congestion of the cortical blood vessels. The renal tubules in the renal cortex and medulla showed degenerative changes of their lining epithelium characterized by mild to moderate vacuolar and hydropic degeneration. Occasionally, the lining epithelium of renal tubules revealed coagulative necrosis characterized by retention of tubular architecture with hypereosinophilic cytoplasm and pyknosis or absence of nuclei. Moreover, hyalinized eosinophilic and cellular casts were detected in the lumen of some renal convoluted tubules. Diffusely, the splenic red pulp was expanded by congested blood vessels and large numbers of erythrocytes.

Multifocally hemorrhages obscured splenic architecture. There is diffuse lymphoid depletion in the white pulp characterized by a marked decrease in size and number of periarteriolar lymphatic sheaths and lymphoid follicles, and remaining follicles lack discernable germinal centers, mantle, and marginal zones.

4. Discussion

4.1. Characterization of iron oxide nanoparticles (Fe_2O_3-NPs)

The X-ray of powder was high purity, clear and sharp peaks, brownish-black pyramidal crystal structure and the average crystal (diameter), that is revert to the cubic phase of IONP, as well, the formation IONP in magnetite phase as conformed by diffraction peaks indexes, according to [17]. Also, the SEM showed the particles are homogeneous distribution, size, and shape, few aggregates, have cluster of small particles that is led to the high surface area and increase surface charges as recently reviewed by [41].

4.2. Hematology, serum analysis, and growth evaluation

The growth performance of albino rats was increased during the feeding on fortified biscuit which helps in IDA treatment due to the high nutritional value of biscuit, the high bio-availability and absorption in small intestinal barrier which depended on the size and conversion of IONP, the ascorbic acid maximize the metabolic pathway of IONP in different rat's tissue with accumulation. These results are according to those obtained by [42]. Moreover, the increased values of CBCs parameters i.e. RBCs, WBCs, Hb, MCV, MCH, MCHC, and PLTs due to the high nutritional value of fortified biscuit with Fe_2O_3-NPs and coated with chocolate, also, the stimulation of erythropoiesis process caused by nano-iron formula as a result of the intestinal efficacy absorption and cellular uptake. That is led to O_2 transport, hemoglobin, red blood cells, and DNA synthesis, ATP production. As well, increase the nutritional quality of proteins in the gut and steroid synthesis and electron transport. Additionally, the excellent biocompatibility, bioavailability, and ability, as well, their ease of synthesis for biomedical applications and treatment of various diseases. These results are similar to with those investigated by [27; 43]

Fig. (5): Effect of feeding basal diet free off nano-iron on spleen, kidney, and liver in anemic group (G4) during feeding period for 6 weeks.

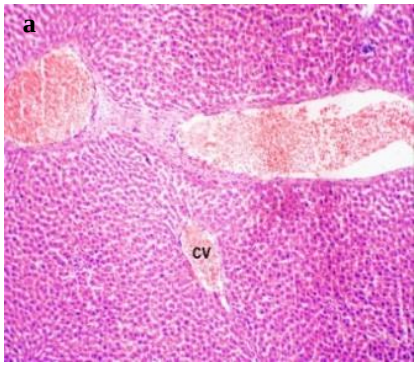

(a): Liver of iron-deficient rat showing marked dilatation and congestion of central veins (CV). H&E stain x 100.

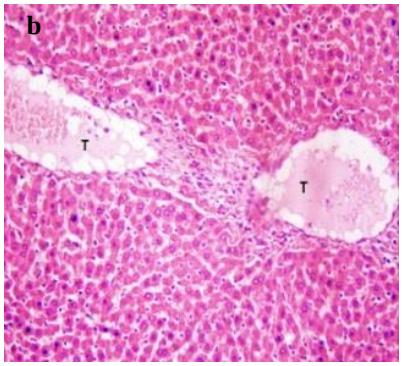

(b): Liver of iron-deficient rat showing fibrin thrombus (T) attached to tunica intima and partially occluded the lumen of central vein. H&E stain x 200.

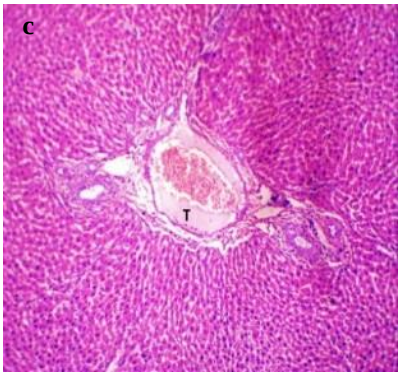

(c): Liver of iron-deficient rat showing fibrin thrombus (T) attached to tunica intima and partially occluded the lumen of portal vein. H&E stain x 100.

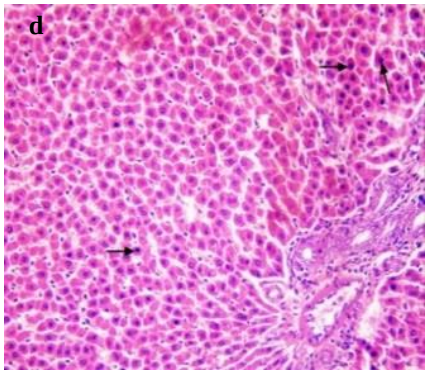

(d): Liver of iron-deficient rat showing coagulative necrosis characterized by loss of cellular detail of hepatocytes and retention of tissue architecture with shrunken hyper eosinophilic cytoplasm and pyknotic nuclei (arrow). H&E stain x 200.

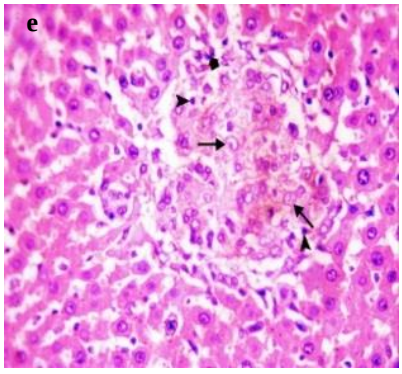

(e): Liver of iron-deficient showing hepatocellular necrosis, with loss of cord architecture and replaced by macrophages (arrow), lymphocytes (arrowhead), neutrophils (thick arrow), fibrin and small amounts of eosinophilic cellular and karyorrhectic debris. H&E stain x 400.

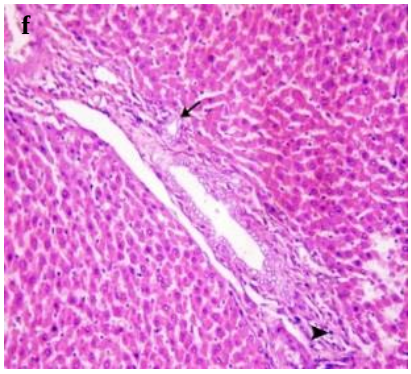

(f): Liver of iron-deficient rat showing increased numbers of small bile ducts (arrow) and low numbers of mononuclear inflammatory cells (arrowhead) in portal area. H&E stain x 200.

Fig. (5 continue): Effect of feeding basal diet free off nano-iron on spleen, kidney, and liver in anemic group (G4) during feeding period for 6 weeks.

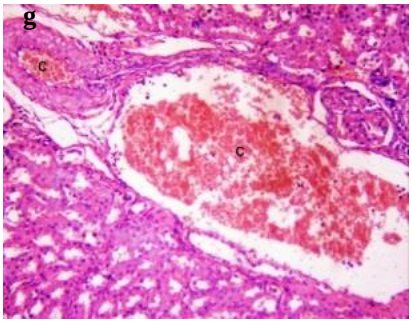

(g): Kidney of iron-deficient rat showing congestion (C) of the cortical blood vessels. H&E stain x 400.

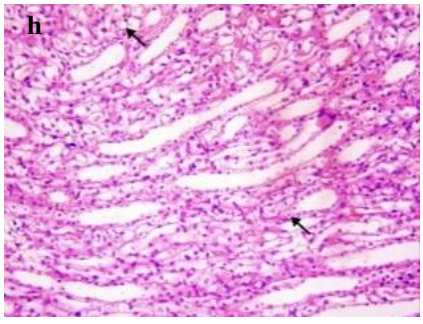

(h): Kidney of iron-deficient rat showing vacuolar and hydropic degeneration (arrow) of lining epithelium of renal tubules in medulla. H&E stain x 200.

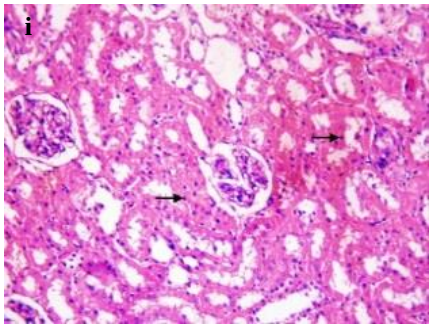

(i): Kidney of iron-deficient rat showing coagulative necrosis of the lining epithelium of renal tubules characterized by retention of tubular architecture with hyper eosinophilic cytoplasm and pyknosis (arrow) or absence of nuclei. H&E stain x 200.

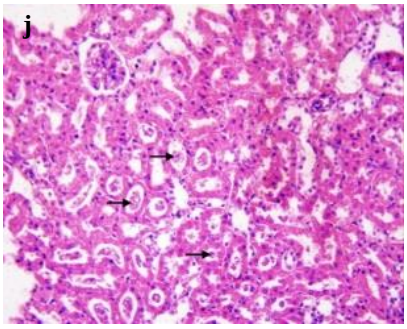

(j): Kidney of iron-deficient rat hyalinized eosinophilic and cellular casts (arrow) in the lumen of some renal convoluted tubules. H&E stain x 400.

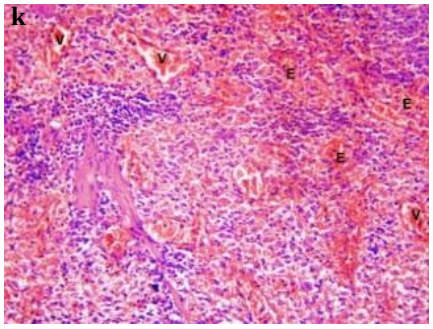

(k): Spleen of iron-deficient rat showing congested blood vessels (V) and large numbers of erythrocytes (E) in red pulp. H&E stain x 400.

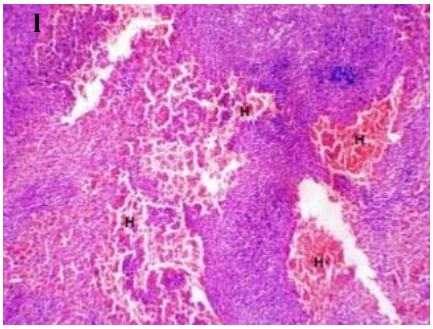

(l): Spleen of iron-deficient rat showing multifocal hemorrhages (H) obscured splenic architecture. H&E stain x 100.

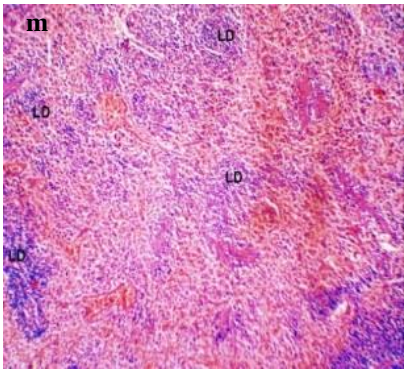

(m): Spleen of iron-deficient rat showing diffuse lymphoid depletion (LD) in the white pulp characterized by a marked decrease in size and number of periarteriolar lymphatic sheaths and lymphoid follicles. H&E stain x 200

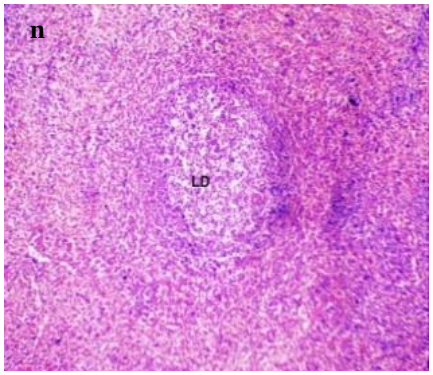

(n): Spleen of iron-deficient rat showing lymphoid depletion (LD) in white pulp with lack discernable germinal centers. H&E stain x 200.

The results of serum analyses such as TIBC, Tf, TI, TP, Na, K, RCs, and GGT revert to the high nutritional value of fortified biscuits. As well, the coating of Fe_2O_3-NPs by ascorbic acid maximizes the absorption and bioavailability of Fe_2O_3-NPs in the small intestine with a low side effect. Additionally, the ascorbic acid absorbed by the M cells and increase the bioavailability of nano-iron to perform it is a vital role. These data are in agreement with those reported by [44-46]

The results of kidney functions such as urea, uric acid, and creatinine referred to as the fortified biscuit plays a vital role in IDA treatment due to its high nutritional value. Moreover, there was not any non-significate effect appeared on the kidney from iron oxide nanoparticles. Additionally, the kidney could not perform its vital role in G4 compared with G3. These findings due to the high absorption of Fe_2O_3-NPs [44; 47]

The liver enzyme e.g. albumin, ALP, GOT, GPT, and total bilirubin back to high level in G4 referred to high IDA. Also, the nano-iron enhanced liver enzyme activity and protein levels. In addition, there is no side effect of fortified biscuit on the liver function in the G3. These data according to those results investigated by [22; 48]

4.3. Histopathological examination

There are no histopathological changes of G1 and G2 due to there is not any bad effect on the different organs caused by feeding on fortified biscuit and basal diet. These results are in agreement with those obtained by [49-50]. Also, the results of G3 back to the safety and high nutrition of fortified biscuit on the different organs, and there was not any side effect on the organ's vital role. These data similar to those investigated by [27; 47]. Additionally, the results of G4 revert to the high iron deficiency anemia in albino rats. Also, the different organs could not play their role because there is a low iron level and IDA. These results are in similar to those obtained by [22; 27].

5. Feasibility of fortified biscuit with nano-iron

Biscuit is a favor, spread, and suitable product for all people around the world due to its cheap, easy absorption, and high nutrition. The cost of a biscuit coated with chocolate in the market for customers (20 g) is US $ 0.5. The price of nano-iron (1g) is US $ 9.3.

The addition ratio of nano-iron is (10 microgram /20g daily). The cost of a fortified biscuit with chocolate incorporated nano-iron is US $ 0.6. While, the price of traditional medical iron solution is US $ 3.1 and takes a long time to increase the iron level in blood. The dimensions 50 mm diameter, thickness 5 mm, and weight 6.5 g of biscuit is So, the functional biscuit incorporated nano-iron is cheap, healthy, highly economic feasibility, high nutrition, and rapidly positive effect compared with traditional medical iron solution according to [25].

6. conclusions

Results showed that biscuit enriched with nano-iron is extremely nutritional value and increase the iron level in blood. As well, it is a novel approach to treat the iron deficiency anemia (IDA) disease, immunity, and pathogens i.e. COVID-19. However, Fe_2O_3-NPs (49.5±5 nm) at 10 ppm were efficient to improve the serum parameters of total iron, total protein, serum sodium and potassium, and reticulocyte counts. As well, it improves CBCs, kidney and liver parameters, growth rate of rats, and there are not non-significant effects on the kidney, spleen, and liver. This study concluded that; the fortified biscuit which is covered by chocolate included Fe_2O_3-NPs (10 ppm) at 49.5±5 nm is more active to overcome iron deficiency anemia disease and increase the iron level in blood. The results demonstrated that the anemic group G3 fed on biscuit enriched with Fe_2O_3-NPs is enhanced the iron level and overcome the IDA compared with other groups. Functional biscuit enriched with nano-iron is preferably for children, elderly, and women to improve their health. Fortified biscuit with Fe_2O_3-NPs is the most feasible and efficient compared with traditional medicine for IDA disease.

7. Acknowledgement

The authors express their sincere gratitude and appreciation for the financial support from the Academy of Scientific Research and Technology in Egypt (ASRT) for their financial support (SNG 5 – 2016). Also, deep thanks to Food Technology Department, Faculty of Agriculture, Benha University for Laboratories support.

8. Author contributions

Osman A wrote the manuscript paper. Osman A and Morsy M designed the experiments. El-Desouky A and Mohamed analysis the obtained data. Aboud A reviewed all manuscript. All authors read and approved the final manuscript.

9. Disclosure statement

The researchers confirm that they have not any competing interests.

10. Funding

This research has been supported by grants (SNG 5 – 2016) from the Academy of Scientific Research and Technology (ASRT), Cairo, Egypt.

11. References

[1] Durán E., Churio O., Arias J.L., Neira-Carrillo A. and Valenzuela C., preparation and characterization of novel edible matrices based on alginate and whey for oral delivery of iron. *Food Hydrocoll.*, **98**, 1–9(2020).

[2] Fathy M.M., Fahmy H.M., Balah A.M.M., Mohamed F.F. and Elshemey W.M., Magnetic nanoparticles-loaded liposomes as a novel treatment agent for iron de fi ciency anemia : In vivo study. *Life Sci.*, **234**, 1–12(2019).

[3] WHO, UNICEF, UNU. 2015. Iron deficiency anemia: assessment, prevention, and control. A guide for programme managers. Geneva, World Health Organization, 2001. WHO/NHD/01.3.http://www.who.int/nutrition/publications/en/ida_assessment_prevention_control.pdf. Accessed March 2015.

[4] Hatefi L. and Farhadian N., A safe and efficient method for encapsulation of ferrous sulfate in solid lipid nanoparticle for non-oxidation and sustained iron delivery. *Colloid Interface Sci. Commun.*, **34**, 1–10(2020).

[5] Rothan H.A. and Byrareddy S.N., The epidemiology and pathogenesis of coronavirus disease (COVID-19) outbreak. *J. Autoimmunity*, **109**, 1–4(2020).

[6] Sanders J.M., Monogue M.L., Jodlowski T.Z. and Cutrell, J.B., Pharmacologic treatments for coronavirus disease 2019 (COVID-19). *J American Med, Assoc.*, **323**(18) 1824–1836(2020).

[7] Di Gennaro F., Pizzol D., Marotta C., Antunes M., Racalbuto V., Veronese N. and Smith L., Coronavirus diseases (COVID-19) current status and future perspectives: A narrative review. *Int. J. Environ. Res. Public Health*, **17**, 1–11(2020).

[8] Cavezzi A., Troiani E. and Corrao S., COVID-19: hemoglobin, iron, and hypoxia beyond inflammation. *Clin. Pract.*, **10**(2), 24–30(2020).

[9] W.H.O. Coronavirus disease (COVID-19) dashboard. https://covid19.who.int/, (2020).

[10] Maciel V.B.V., Yoshida C.M.P., Boesch C., Goycoolea F.M. and Carvalho R.A., Food hydrocolloids iron-rich chitosan-pectin colloidal microparticles laden with ora-pro-nobis (*Pereskia aculeata Miller*) extract. *Food Hydrocoll.*, **98**, 1–12(2020).

[11] Hamano H., Niimura T., Horinouchi Y., Zamami Y., Takechid K., Godab M., Imanishib M., Chumad M., Izawa-Ishizawae Y., Miyamotof L., Fukushimag K., Fujinog H., Tsuchiyaf K., Ishizawaa K., Tamakic T. and Ikeda Y., Proton

pump inhibitors block iron absorption through direct regulation of hepcidin via the aryl hydrocarbon receptor-mediated pathway. *Toxicology Letters*, **318**, 86–91(2020).

[12] National Health Institutes, Iron, vitamins, and minerals. https://www.nhs.uk/conditions/vitamins-and-minerals/iron/ (2020).

[13] Kohgo Y., Ikuta K., Ohtake T., Torimoto Y. and Kato J., Body iron metabolism and pathophysiology of iron overload. *Int.l J. Hematolo.*, **88**(1), 7–15(2008).

[14] Sharp P. and Kaila S.K., Molecular mechanisms involved in intestinal iron absorption. *World J. Gas.*, **13**(35), 4716–4724(2007).

[15] Yiannikourides A. and Latunde-Dada G.O., A short review of iron metabolism and pathophysiology of iron disorders. *Medicines*, **6**(85), 1–15(2019).

[16] Ebner N. and Von H.S., Iron deficiency in heart failure: a practical guide. *Nutrients*, **5**(9), 3730–3739(2013).

[17] Hashem F., Nasr M. and Ahmed, Y., Preparation and evaluation of iron oxide nanoparticles for treatment of iron deficiency anemia. *Int. J. Pharm. and Pharm. Sci.*, **10**(1), 142–146(2018).

[18] Wang X., Zhang M., Flores S.R.L., Woloshun R.R., Yang C., Yin L., Xiang P., Xu X., Garrick M.D., Vidyasagar S., Merlin D. and Collins J.F., Oral gavage of ginger nanoparticle-derived lipid vectors carrying dmt1 siRNA blunts iron loading in murine hereditary hemochromatosis. *Molecular Therapy*, **27**(3), 493–506(2019).

[19] Jubran A.A., Al-Zamely O.M. and Al-Ammar M.H., Estimation of iron oxide nanoparticles on white albino mice induced with iron deficiency anemia. *Drug Invention Today*, **11**(11), 2880–2886(2019).

[20] Garcés V., Rodriguez-nogales A., Gonzalez A., Gálvez N., Rodriguez-cabezas E., Gutiérrez L., Rondon D., Olivares M., Galvez J. and Dominguez-vera, J., Bacteria-carried iron oxide nanoparticles for treatment of anemia. *Bioconjugate Chem.*, **2018**, 1–24(2018).

[21] Dasgupta N. and Ranjan S., An Introduction to Food Grade Nanoemulsions. Environmental chemistry for a sustainable world (e book), Springer, 151–174(2018).

[22] Kandasamy G., Sudame A., Luthra T., Saini K. and Maity D., Functionalized hydrophilic superparamagnetic iron oxide nanoparticles for magnetic fluid hyperthermia application in liver cancer treatment. *ACS Omega*, **3**, 3991−4005(2018).

[23] Peter-Ikechukwu A.I., Omeire G.C., Kabuo N.O., Eluchie C.N., Amandikwa C. and Odoemenam G.I., Production and evaluation of biscuits made from wheat flour and toasted watermelon seed meal as fat substitute. *J. Food Res.*, **7**(5), 112–123(2018).

[24] Canali G., Balestra F., Glicerina V., Pasini F., Caboni M.F. and Romani S., Influence of different baking powders on physico-chemical , sensory and volatile compounds in biscuits and their impact on textural modifications during soaking. *J. of Food Sci. and Technolo.*, **2020**, 1–10(2020).

[25] El-Bahr S.M., Elbakery A.M., El-Gazzar N., Amin A.A., Al-Sultan S., Alfattah M.A., Shousha S., Alhojaily S., Shathele M., Sabeq I.I. and Hamouda A.F., Biosynthesized Iron Oxide Nanoparticles from *Petroselinum crispum* Leaf Extract Mitigate Lead-Acetate-Induced Anemia in Male Albino Rats: Hematological, Biochemical and Histopathological Features. *Toxics*, **9**(123), 1–17(2021).

[26] Mazgaj R., Lipi´nski P., Szudzik M., Jo´nczy A., Kope´c Z., Stankiewicz A.M., Kamyczek M., Swinkels D., Zelazowska B. and Starzy´nski R.R., Comparative Evaluation of Sucrosomial Iron and Iron Oxide Nanoparticles as Oral Supplements in Iron Deficiency Anemia in Piglets. *Int. J. Mol. Sci.*, **22**(9930), 1–20(2021).

[27] Salaheldin T.A. and Regheb E.M., In-vivo nutritional and toxicological evaluation of nano iron fortified biscuits as food supplement for iron deficient anemia. *J. of Nanomedicine Res.*, **3**(1), 1–9(2016).

[28] Akbari B., Tavandashti M.P. and Zandrahimi M., Particle size characterization of nanoparticles- a practical approach. *Iran. J. Mater. Sci. Eng.*, **8**(2), 48–56(2011).

[29] Alwan L.H. and AL JEBUR L., Studying the effect of gold nanoparticles on mixture of surfactant of sodium
dodecyl benzene sulfonate (SDBS) surfactant and folic acid. *Egypt. J. Chem.*, **65**(3), 385–394(2022).

[30] de Moura M.R., Aouada F.A., Avena-Bustillos R.J., McHugh T.H., Krochta J.M. and Mattoso L.H.C., Improved barrier and mechanical properties of novel hydroxypropyl methylcellulose edible films with chitosan/tripolyphosphate nanoparticles. *J. Food Eng.*, **92**(4), 448–453(2009).

[31] A.O.A.C. Association of Official Analytical Chemists. Official Methods of Analysis. (20th Ed.) Maryland, USA. (2016).

[32] Lee H.W., Kim H., Ryuk J.A., Kil K. and Ko B.S., Hemopoietic effect of extracts from constituent herbal medicines of Samul-tang on phenylhydrazine-induced hemolytic anemia in rats. *Int. J. Clin. Exp. Pathol.*, **7**(9), 6179–6185(2014).

[33] Dawood M.A.O., Zommarab M., Eweedaha

N.M. and Helal A.I., The evaluation of growth performance, blood health, oxidative status and immune-related gene expression in Nile tilapia (*Oreochromis niloticus*) fed dietary nanoselenium spheres produced by lactic acid bacteria. *Aquaculture*, **515**, 1–10(2020).

[34] Maldiney T., Bessière A., Seguin J., Teston E., Sharma S.K., Viana B., Bos A.J.J., Dorenbos P., Bessodes M., Gourier D., Scherman D. and Richard C., The in vivo activation of persistent nanophosphors for optical imaging of vascularization, tumours and grafted cells. *Nature Mat.*, **13**, 418–426(2014).

[35] Wuyts B., Delanghe J.R., Kasvosve I., Wauters A., Neels H. and Janssen S.J., Determination of carbohydrate-deficient transferrin using capillary zone electrophoresis. *Clini. Chem.*, **47**(2), 247–255(2001).

[36] Yanardag R. and Ozsoy-sacan O., Combined effects of vitamin c, vitamin e, and sodium selenate supplementation on absolute ethanol-induced injury in various organs of rats. *Int.J.Toxicolo.*, **26**, 513–523(2007).

[37] Sidhu G.K., Malek R.R., Khubchandani A., Mansuri S.H., Patel M.S. and Oza R.H., A Study of Serum Urea, Creatinine and Uric Acid Levels In Hypothyroid Patients. *Int. J. Res. Med.*, **5**(2), 115–118(2016).

[38] Bais B. and Saiju A., Meliorative effect of Leucas cephalotes extract on isoniazid and rifampicin induced hepatotoxicity. *Asian Pac. J. Trop. Biomed.*, **4**(2), 633–638(2014).

[39] Mishra S.U., Pandey C.M., Mishra P. and Pandey G., Application of Student's t-test, Analysis of Variance, and Covariance. *Ann.Card Anaesth*, **22**:407–11(2019).

[40] da Silva T.F. and Conti-Silva A.C., Potentiality of gluten-free chocolate cookies with added inulin/oligofructose: Chemical, physical and sensory characterization. *LWT - Food Sci. and Technolo.*, **90**, 172–179(2018).

[41] Karimzadeh I., Dizaji R.H.G. and Aghazadeh M., Electrochemical synthesis and characterization of α -Fe_2O_3 nanoparticles. 3rd International Conference on Nanotechnology (ICN2015), 27-28 August 2015, Istanbul, Turkey. (2016).

[42] Elsayed H.H., Al-sherbini A.S.A.M., Abd-elhady E.E. and Ahmed K.A., Treatment of anemia progression via magnetite and folate nanoparticles in vivo. *ISRN Nanotechnology*, **2014**, 1–13(2014).

[43] Jimenez K., Kulnigg-dabsch S. and Gasche C., Management of iron deficiency anemia. *Gastroenterol. Hepatolo.*, **11**(4), 241–250(2015).

[44] Elshemy M.A., Iron oxide nanoparticles versus ferrous sulfate in treatment of iron deficiency anemia in rats. *Egyptian J. of Vet. Sci.*, **49**(2), 103–109(2018).

[45] Ghio S., Fortuni F., Capettini A.C., Scelsi L., Greco A., Vullo E., Raineri C., Guida S., Turco A., Gargiulo C. and Visconti L.O., Iron deficiency in pulmonary arterial hypertension : prevalence and potential usefulness of oral supplementation usefulness of oral supplementation. *Acta Cardiologica*, **1**, 1–6(2019).

[46] Shafie E.H., Keshavarz S.A., Kefayati M.E. and Taheri F., The effects of nanoparticles containing iron on blood and inflammatory markers in comparison to ferrous sulfate in anemic rats. *Int. J. Preventive Med.*, **3**, 1–7(2019).

[47] Koutroubakis I. E., Oustamanolakis P., Karakoidas C., Mantzaris G. J. and Kouroumalis E. A., Safety and efficacy of total-dose infusion of low molecular weight iron dextran for iron deficiency anemia in patients with inflammatory bowel disease. *Dig. Dis. Sci.*, **55**, 2327–2331(2010).

[48] Benyettou F., Ocadiz A., Ravaux F., Rezgui R., Jouiad M., Nehme S.I., Parsapur K. and Olsen J., Mesoporous g-iron oxide nanoparticles for magnetically triggered release of doxorubicin and hyperthermia treatment. *Chem. Euro. J.*, **22**, 1–10(2016).

[49] Saffari S., Keyvanshokooh S., Zakeri M., Johari S.A., Pasha-Zanoosi H. and Mozanzadeh M.T., Effects of dietary organic, inorganic, and nanoparticulate selenium sources on growth, hemato-immunological, and serum biochemical parameters of common carp *(Cyprinus carpio)*. *Fish Physiol, Biochem.*,**44**, 1087–1097(2018).

[50] Shirsat S., Kadam A., Mane R.S., Jadhav V.V., Zate M.K., Naushad M. and Kim K.H., Protective role of biogenic selenium nanoparticles in immunological and oxidative stress generated by enrofloxacin in broiler chicken. *Dalton Trans.*,**45**, 8845–8853(2016).